PHYSICS WITH LINEAR COLLIDERS IN THE TEV CM ENERGY REGION

F. Bulos[†], V. Cook[*], I. Hinchliffe[**], K. Lane[††],

D. Pellet[⊗], M. Perl[†], A. Seiden[Δ], H. Wiedemann[†]

I. Introduction

It may well be that the e^+e^- physics beyond PEP and PETRA and and up to 200 GeV CM energy will deal primarily with the verification of the standard model (SM) of weak and electromagnetic interactions. Various theoretical and experimental studies at workshops for contemplated accelerators[1] (SLC, LEP I, Z^0 at Cornell) have assumed this.

Beyond 200 GeV the picture is less clear. The absence of theoretical models with strong predictions comparable to the SM adds to the difficulty. In addition, the experimental verification of the SM itself is yet to come, and one is forced to make certain assumptions about the outcome.

Here we join some our colleagues in previous studies[2] (in particular J. Ellis and I. Hincliffe) in making the following assumptions:

1) Z^0, $W^\pm$, light higgs (if $M_H < 100$ GeV) have all been discovered.

2) The t quark has been discovered if its mass is < 100 GeV.

3) QCD is basically the correct theory of the strong interactions.

With these assumptions, we have produced an updated table of possible physics in the TeV region (Table I). This table was used as the basis for the study of specific physics below. It contains best estimates of cross-section, promising signatures for final states, and some helpful comments.

As customary we have used σ (point) = 1 unit of R as the unit of cross-section:

$$\sigma \text{ (point)} \approx \frac{87}{(E_{CM}(\text{GeV}))^2} \text{ nb}$$

At E of 700 GeV:

$$\sigma \text{ (point)} \approx 1 \text{ unit of R} = 1.8 \times 10^{-37} \text{cm}^2 \quad .$$

The CM energy of 700 GeV was selected here from the range of energies contemplated for linear colliders (see colliders section). At this energy a luminosity

of $10^{33} \text{cm}^{-2}\text{sec}^{-1}$ is attainable with relatively modest AC power, and an energy spread $\Delta E/E < 5\%$.

At this energy and luminosity:

σ (point) = 1 unit of R ≡ 15 events/day.

II. Physics-General

Before we go into specifics, some general observations can be made after a glance at Table I.

1) If we exclude the $Z^{0'}$ then the direct production of Z^0Z^0, W^+W^- and the 3 generations of quarks constitute a major part of the cross-section (∿ 35 units of R). They also are the major byproducts of the new physics. Thus the direct production of the "known" physics constitutes a background to the study of the new physics. Two photon processes are also a potential background (see later).

2) The new physics yields a large number of jets containing ordinary light hardrons. If one ignores light hardron masses, the situation looks like π^0, η physics at SPEAR energies with hadronic jets from Z^0, W replacing γ's from π^0, η. By analogy it is expected that the reconstruction of Z^0, W from pairs of jets would be very useful in understanding events in the TeV region. In Appendix A we discuss di-jets at the W-mass.

3) Except for $Z^{0'}$, most specific final states have cross-sections of the order of 1 unit of R.

4) There are a few prominent signatures which characterize the new physics

a) Large No. of jets 6-8 (Ex: $H^{0'}$ production) with di-jet masses at Z^0, W mass.

b) High momentum leptons isolated in phase space (Ex: $\tilde{\ell} \tilde{\ell}$ production).

c) Large missing energy and momentum pointing into detector accompanying jets (Ex: $L \bar{L} \rightarrow \nu \bar{\nu} W^+ W^-$, the W-pair giving 4 jets, or isolated leptons as in b) above). We can get an idea of the rejection one obtains against $q \bar{q}$ states from Fig. 1 (borrowed from SLC workshop). For ∿ 4π solid angle acceptance, a factor of 100 rejection is obtained by requiring > 25% missing energy for the ν case. Requiring an isolated charged lepton (no nearby hadrons) gives a factor > 100 if we require it to have > 25% of the energy.

Finally we would like to stress the difference between detecting the presence of new physics and establishing its parameters. For example the presence of 8 high energy jets separated in space is a good signature for heavy Higgs production. However, establishing the Higgs mass requires a few hundred such events to enable the reconstruction of di-jets into Z^0, $W^\pm$, and the subsequent reconstruction of the Higgses from Z^0, W pairs.

---

† : Stanford Linear Accelerator Center, Stanford, CA 94305

* : University of Washington, Seattle, WA

** : Lawrence Berkeley Laboratory, Berkeley, CA

†† : Ohio State University, Columbus, Ohio 43210

⊗ : University of California, Davis, CA

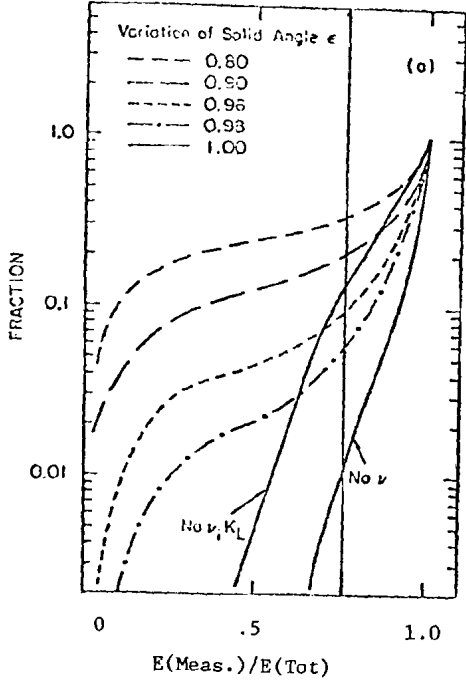Δ : University of California, Santa Cruz, CA 95064

Fig. II.1: From SLC Workshop
page 225.

III. Physics - Specific

We turn now to the discussion of specific final states (selected from Table I), their competing backgrounds, and running times required to study them. What follows is by no means exhaustive. It is meant to illustrate the scale of physics at TeV $e^+ e^-$ colliders.

We start first with resonances, namely $Z^{0'}$, heavy quarkonia, ρ_T (Techni-Rho). Using Table I and Ref. 2(c) we construct a subtable Table II.

1. $\underline{Z^{0'}}$. Table II shows that $Z^{0'}$ is produced at the rate of 75,000/day at the peak, while the remainder in the table amounts to 850/day. A quick scan in the region of 200 → 700 GeV CM in steps of 5 GeV (100 steps) is sufficient to find the $Z^{0'}$. With $Z^{0'}$ width $\sim$ 3% and ($\Delta E/E$) beam $\sim$ 5%, the effective R at resonance is reduced by a factor $\dfrac{3}{2 \times 5}$ = .3, hence the effective rate of $Z^{0'}$ production is $\sim$ 23000/day. With two hours spent at each step, then:

$Z^{0'}$ produced at $Z^{0'}$ mass/2 hrs = 2000

Background/2 hrs = 70

Such an increase above background is easily detectable and is sufficient to map the shape of Z^0 resonance.

Total time for scan $\simeq$ 10 days.

2. Technicolor. Here, a spin-one technihadron called ρ_T appears as an s-channel resonance in e^+e^- annihilation. Its mass is expected to be $M_{\rho T} \cong$ 700-900 GeV and its width $\Gamma_{\rho_T} \cong$ 250-400 GeV. At the resonance peak, $\Delta R \cong 10$-20 (see Fig. 2). The most efficient way to search for ρ_T is to measure $R(e^+e^- \to$ hadrons including, possibly, isolated leptons) at $\sqrt{s} \cong$ 400 GeV and 1000 GeV. Technicolor should give $\Delta R \cong$ 5-10 over this range. If this is observed, one then searches for ρ_T in a "binary" scan, alternating

between high and low energies to zero in on the peak. This search should require 20-30 days.

In most technicolor models, ρ_T decays exclusively to a variety of pairs of charged technipions (whose masses range from 10 to 250 GeV) and pairs of longitudinally-polarized charged weak bosons, $W_L^+ W_L^-$. The decay anglular distribution is proportional to $\sin^2\theta$. One particular model is analyzed in detail in Ref. 3. There, one expects $\sim$ 3 x 10^4 pairs produced at the resonance peak in 10^7 sec. All events are quite spectacular and it is relatively easy to distinguish among the various decay modes of ρ_T.
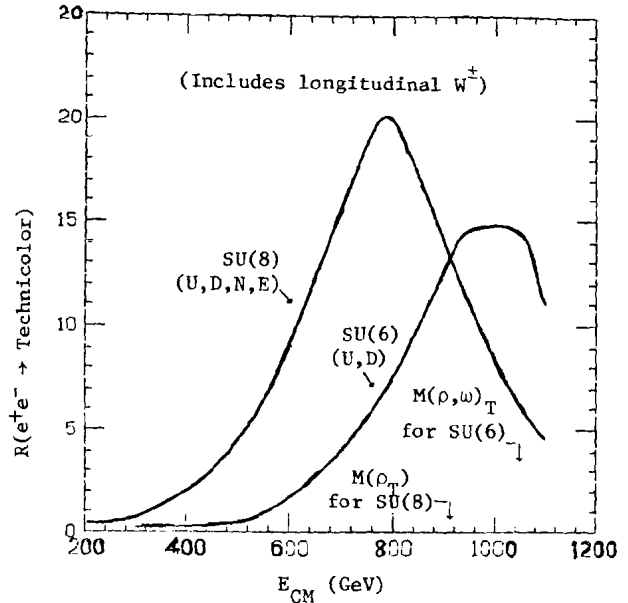

Fig. III.1: Technicolor production in two
models. Courtesy of M. Peskin
(This Proceedings).

3. Heavy Quarkonia: These resonances are broadened by the decay $Q \to q + W$ amd $Q \to H^{\pm} + q$ such that they merge into a continuum. The best signatures are the rise in R and/or the change in sphericity. Both suggest a scan. However, to detect 2 units rise in R with the 5σ criteria requires $\sim$ 15 days/pnt using the solid angle cut discussed below, or $\sim$ 35 days/pnt without the cut.

The next distinctive signature is the presence of 6 jets from the weak decay above, with two groups (of 3 jets each) back to back. The most serious background is 30 units of R of Z^0Z^0, W^+W^- production (Table I). As suggested in Ref. 2(c) a cut on solid angle of cos $\theta \leq$ .8 leave 5 units of R. However, this final state contains 4 jets. The probability for a quark jet to become 2 jets by gluon emission is $\sim \alpha_s$, hence the probability for a pair of Z^0 or W's to give 6 jets is $\simeq$ .2. The background then amounts to 1 unit or R i.e. signal to noise $\simeq$ 2/1. For Q production one then requires two of the 3 jets on each side to reconstruct the mass of W. It is hard to estimate the running time required for this technique. However this analysis can be done while searching for other final states (Ex: the scan for ρ_T above).

We look, next, at nonresonant final states:

4. Heavy Higgs $\underline{H^{0'}}$: The β^3 dependence of cross section suggests that in searching for these particles one should sit at the highest energy available. The best signature is the large number of jets or jets and leptons with di-jet masses at W, Z^0 mass and di-lepton

mass at the Z^0 mass. This signature is relatively background free. The probability that all the decay products are jets and lepton pairs is $\simeq 10\%$ averaged over neutral and charged Higgses. From Table I the cross section is $\simeq .2$ unit of $R \equiv .3$ events/day at the 10% efficiency above. A year of running will yield ≈ 110 such events. This might be enough to use the di-jet mass technique and to reconstruct the Higgs mass. It is not necessary that this be all dedicated running. Once again the search for the 6 jets can be done in conjunction with other searches.

5. <u>Supersymmetrics</u> : For example consider scalar muon pairs $(\tilde{\mu} \tilde{\mu} \rightarrow \mu \tilde{\mu} \tilde{\gamma} \tilde{\gamma})$. The signature is a lepton pair with missing energy. The background is $W^+W^- \rightarrow \mu^+\nu \ \mu^-\bar{\nu}$. W pairs are produced at 24 units of R. From Ref. 2(c) a cut on solid angle at 80% leaves 4 units of R. For three generations the BR $W \rightarrow e\nu$ is 1/12. Hence the background is $4/(12)^2$ units of R = .03 while the signal is $\simeq .5$ units (sig./BG ≈ 17). In two months of running a signal of ≈ 400 events are obtained with 6% contamination. To establish that a scalar muon was produced might require mapping out the β^3 and $\sin^2\theta$ dependence of the production cross section. For more details see Refs. 4, 5.

Another supersymmetric state of interest is $\tilde{q} \ \tilde{q}$ with $\tilde{q} \rightarrow qq\bar{q} \ \tilde{\gamma}$. The signature is 6 jets with large missing energy. As we have seen, heavy Higgs production can yield 6 yets but with no missing energy. However to establish that the origin of these jets is $\tilde{q} \ \tilde{q}$ production is difficult. One indication would be that Z^0's and W's are not involved i.e. the process is not an electro-weak process. For example if in addition to the absence of missing energy none of the di-jet masses were found to be at the Z^0 or W mass.

6. <u>Electron Compositeness</u>: If the electron is a composite object with inverse size Λ, this fact must be reflected in a deviation of the Bhabha scattering cross section from the electroweak expectation[6]. The deviation will be of order (s or t)$/\alpha\Lambda^2$; see references 7, 8.

Thus, the best way to search for electron substructure is to plot, as a function of $\cos\theta$, the fractional deviation of the measured Bhabha cross-section from the electroweak one:

$$\Delta_{ee}(\cos \ \theta) = \frac{d\sigma(e^+e^- \rightarrow e^+e^-)/d(\cos \ \theta)\big|_{\text{meas}}}{d\sigma(e^+e^- \rightarrow e^+e^-)/d(\cos \ \theta)\big|_{\text{EW}}} - 1 \ .$$

The fact that this always vanishes in the forward direction allows one to normalize the measured cross section to the electroweak prediction at small θ. Assuming $\mathcal{L} = 10^{33}\text{cm}^{-2}\text{sec}^{-1}$ at $\sqrt{s}$ = 700 GeV, a 5% (statistical) measurement of the Bhabha cross section would take $1-4 \times 10^6$ seconds per measured point. A true 5% measurement over the range $|\cos \ \theta| \leq 0.8$ should take 1-2 years at most[9].

To see what this means in terms of setting limits on substructure, we have determined values of Λ which give $0.5 \lesssim |\Delta_{ee}| \lesssim 0.10$ over a large angular range. This was done for several choices of the space-time structure of the effective $\bar{e}e\bar{e}e$ interaction induced by compositeness. The results for the most pessimistic and most optimistic cases are shown in Figs. 3a and 3b, respectively. We see that a 5% cross section measurement sets the following limits on Λ:

$\Lambda > 16$ TeV   (left-left model)

$\Lambda > 30$ TeV   (vector-vector or axial-axial model)

Finally, we mention that, as $\sqrt{s}$ approaches Λ, the Bhabha cross section grows like s/Λ^4 at all angles, and ultimately flattens out to the "strong-interaction" goemetric cross section $\sim 1/\Lambda^2$.
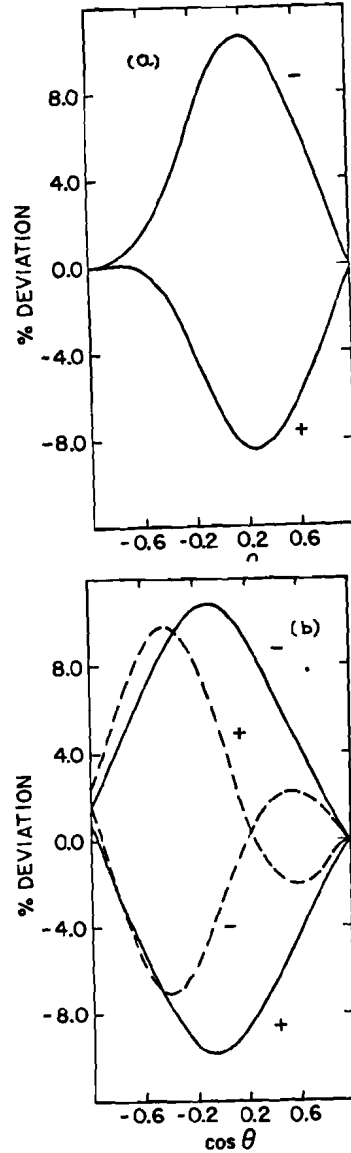

Fig. III.2: The deviation Δ_{ee}, in per cent, of the measured Bhabha cross section from the electroweak one, assuming electron compositeness at scale Λ.

(a) The effective interaction is $(4\pi\alpha/2\Lambda^2)\bar{e}_L\gamma_\mu e_L$ $\bar{e}_L\gamma_\mu e_L$, with Λ = 16 TeV. A right-right model gives nearly identical results at these energies.

(b) The effective interactions are $(4\pi\alpha/2\Lambda^2)\bar{e}\gamma_\mu$ $\bar{e}e\gamma^\mu e$, with Λ = 32.5 TeV (solid lines) and $(4\pi\alpha/2\Lambda^2)\bar{e}\gamma_\mu\gamma_5\bar{e}e\gamma^\mu\gamma_5e$, with Λ = 27.5 TeV (dashed lines).

The $\pm$ signs refer to a = $\pm$ 1.

IV. 2γ Background

A potential background to the e^+e^- annihilation physics is the two photon process which has a nearly energy independent total cross section. Fortunately only a few of these events yield hadronic final states which have invariant masses $\sim \sqrt{s}$ as could be selected by a calorimeter for example. To estimate this background we have used Vermaseren[10] monte carlo program to calculate the process,

$$e^+ e^- \rightarrow e^+ e^- \mu^+ \mu^-$$

via the 6 contributing Q.E.D. diagrams. The rate into $q\bar{q}$ is related to μ pair rate by

$$\sigma\,(e^+e^- + \text{Hadrons}) = (\sum_{\substack{\text{color} \\ \text{flavor}}} Q_i^4)\sigma(e^+e^- + \mu^+\mu^-)$$

If we require that each μ have an energy > 0.8 E(Beam) plus coplanarity cuts then $\sigma(e^+e^- + \mu^+\mu^-) \sim 0.23 \times 10^{-39} \text{cm}^2$. This gives $\sigma(e^+e^- + q\bar{q}) \approx 0.3 \times 10^{-39}\text{cm}^2$ which is $\sim 10^{-3}$ units of R. Even with less stringent energy cuts the two photon background remains tolerable provided reasonable calorimetry is available.

V. Luminosity Monitor

It is clear from the physics section that at least a reasonable relative luminosity monitor is required. Bhabha's at measurable forward angles are too few at these energies. Large angle Bhabhas and μ-pair production in addition to being small is also model dependent. Probably the most promising monitor is W pair production which amounts to 20 units of R. The W pair is recognized by two di-jets back to back each with a mass $= M_W$. Other types of luminosity monitor might develop as we gain experience with colliders.

VI. Conclusion

For most of the physics topics discussed, e^+e^- provides a good production channel. Rates are typically adequate, although a luminosity of $\geq 10^{33}\text{cm}^{-2}\text{sec}^{-1}$ will be needed. Signal/background ratios are substantially larger than those in hadron machines. e^+e^- colliders with such luminosity is the subject of the next section.

Final states tend to be complicated. The best signatures are multijets and isolated leptons, both quite often accompanied with missing energy carried by non-interacting particles. A nearly 4π solid angle calorimeter with good segmentation will be needed to reconstruct multijet invariant masses and to identify electrons and muons. Particles inside a jet will be closely spaced (a typical two particle angular separation $\sim 1^{\circ}$) making tracking inside a jet very difficult. However physics such as was described above can be analysed using whole jets as units, therefore it need not suffer from the lack of detailed tracking.

VII. THE ACCELERATOR

Introduction

To extend the center of mass energies well beyond LEP energies we follow the idea[11] and the expectations[12,17] of colliding linac beams. The second ICFA study[13] has concluded that "storage rings appears to be impossible for energies above 200 GeV per beam." In a linear colliding-beam facility, we face no basic limitation to extend the beam energy far beyond LEP energies. The luminosity too is not limited by physics but rather by economic reasons, since the luminosity is limited only by the electrical power available to the facility.

The principle of a colliding linac beam facility is as follows: Two linear accelerators, one for the electron beam and one for the positron beam, face each other on the same axis. Both linacs are triggered simultaneously, and both beams, after being accelerated and focused down to a small cross section collide at the interaction point. After the collision the beams are disposed of since they are not useful any more for further collisions. This mode of operation avoids the negative effects of the so-called beam-beam interaction which limits the luminosity in storage rings. In linear colliders we are actually aiming for a large beam-beam effect. The focusing effect of one beam on the other can, if strong enough, reduce the effective beam cross section and enhance the luminosity by up to a factor 6. This is what we call the pinch effect in linear collider facilities.

From the principles of linear colliders it is immediately obvious that the luminosity for a particular facility is limited only by the pulse repetition rate of the linear accelerators.

In this section we will describe the parameters of a high-energy linear collider facility to reach center-of-mass energies of 400 to 2000 GeV. In the course of the discussion we will encounter design specifications which have not yet been demonstrated in a real accelerator and are therefore subject to R&D effort. The idea of this section is not to demonstrate the economic feasibility of colliding linac beams with present-day technology but rather to emphasize the possibilities opened up by the idea of colliding linac beams to reach high center-of-mass energies and luminosities for e^+e^- physics.

Many of the crucial parameters are being investigated and pushed to their limits at SLAC in preparation of the SLC project.[18] Should the SLC project become funded it would function not only as a tool to explore the Z_0 physics but also be the prototype of a colliding linac beam facility. Crucial parameters could be studied and limitations thereof be found.

In this report we assume that the SLC is operating at or close to its design performance. We also assume that certain R&D efforts to develop special rf-power sources and high-gradient accelerating sections are successful. All these efforts are not so much necessary to prove the principle but rather to make linear colliders economically feasible.

Linear colliders offer several properties that might be useful for high-energy physics experiments:

- high polarization of the electron beam in any direction is available at very low cost and for every experimental area.

- polarization of the positron beam is possible but at some cost since a long undulator is required to produce polarized gammas which in turn produce polarized positrons in a target.

- a switch from e^+e^- to e^-e^- collisions is very easy to perform however at a loss of luminosity since there is no pinch effect any more.

- e-p collisions are immediately available by the addition of a 30 to 50-GeV proton injector.[16] Above that energy a linear accelerator works the same way for protons as for electrons.

- while one of the beams after collision is used to reproduce positrons, the other beam is available for fixed target or beam dump experiments.

- more exotic collision like γγ or γe have been suggested.[19]

Design Goals

The physics as described in previous sections calls for maximum center-of-mass energies of at least 1000 GeV and possibly above. We will therefore explore the parameters of linear colliders from about 400 GeV up to 2000 GeV. As we mentioned before, the luminosity is limited by the electrical power available to the collider. In this study we have arbitrarily assumed a maximum electrical power of

$$P_{AC} = 100 \text{ MW} \qquad (VII.1)$$

available to the facility limited only by budgetary or environmental considerations. With the luminosity being proportional to this power we will calculate and discuss the parameters required to still reach a luminosity of

$$\mathscr{L} = 10^{33} \text{cm}^{-2}\text{sec}^{-1} \text{ at } E_{c.m.} = 1000 \text{ GeV}$$
$$(VII.2)$$

This is the luminosity into one experiment only while the others would not get any luminosity. Up to four experiments, however, could receive each a quarter of this luminosity. Linear Colliders give the opportunity to give all available luminosity to running detectors only.

This flexibility is available by accelerating up to four bunches simultaneously in the linacs at no extra power cost since only a small fraction of the electrical power is transferred to each bunch. By proper phasing of the accelerating field in the linac sections all four bunches can reach the same experimental area. By a different way of phasing, it can be arranged that all four bunches have slightly different energies and a deflecting magnet at the end of the linac will guide each bunch to a different experiment. With the proper phazing the above total luminosity can be divided among the active experiments at a variety of energies. The options seem to be limitless.

Scaling Laws

The luminosity in a linear collider is given by

$$\mathscr{L} = \frac{N^2 \nu_{rep}}{4\pi\sigma_y^2 R} n_b \cdot p = \mathscr{L}_0 n_b p, \qquad (VII.3)$$

where N is the number of particles per bunch, ν_{rep} is the pulse repetition rate, $4\pi\sigma_y^2 R = 4\pi\sigma_y \cdot \sigma_x$ is the beam cross section, R the aspect ratio, n_b the number of bunches per beam to collide in one interaction point per linac pulse, and p the luminosity enhancement factor

due to the pinch effect.

The luminosity enhancement factor p is determined by the so-called beam disruption parameter

$$D = \frac{2r_e N\sigma_\ell}{\gamma\sigma_y^2(1+R)} \qquad (VII.4)$$

(σ_ℓ bunch length) as shown in Fig. VII.1. The transverse electromagnetic forces exerted on any particle by the other beam causes this particle to emit
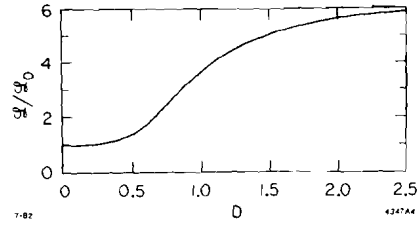

Fig. VII.1: Luminosity Enhancement Factor $p = \mathscr{L}/\mathscr{L}_0$ as a Function of the Disruption Factor.

synchrotron radiation which is called beam strahlung. This in turn increases the energy spread in the beam by [21]

$$\frac{\Delta E}{E} = \frac{2r_e^3}{3} \frac{N^2}{\sigma_y^2 R\sigma_\ell} \gamma F(R), \qquad (VII.5)$$

with

$$F(R) = \frac{4}{\sqrt{\pi}} \frac{1}{R\sqrt{P}} \begin{cases} 2 \text{ atan } (\sqrt{P}/Q) \text{ for } P > 0 \\ \ln \dfrac{1+\sqrt{P}/Q}{1-\sqrt{P}/Q} \text{ for } P < 0 \end{cases}$$
$$(VII.6)$$

and $P = 3/R^4 - 10/R^2+3$; $Q = 3/R^2 + 8/R+3$. This energy spread has to be limited depending on the kind of experiment performed at the linear collider.

The number N of particles per bunch is limited by wake field effects in the linear accelerator. A beam that passes a linac section with a small transverse displacement excites modes with nonzero fields in the center of the accelerating structure. In particular the fields generated by the head of the bunch act back on the tail of the bunch and increase the beam size. The effect on the beam depends on the beam alignment, the gradient (g), and the ratio of the final energy (E) to the injection energy (E_0). These effects have been calculated in the SLC case for an rms beam displacement of .1 mm. The increase in normalized beam emittance is $\Delta\epsilon\gamma = 3 \times 10^{-6}$m-r, and the resulting scaling factor A determining N is [22,23]

$$A = \frac{N\cdot\ln(E/E_0)}{g} = 1.5\cdot10^{10} \frac{m}{MeV} . \qquad (VII.7)$$

The final boundary condition we want to observe is the total power available to run the rf system of the linear collider.

$$P_{AC} = 2\frac{1}{\eta} \frac{2\tau}{1-e^{-2\tau}} \frac{gE}{\omega_{rf}\frac{r}{Q}} \nu_{rep} = \alpha gE\nu_{rep}. \qquad (VII.8)$$

($\alpha = 3.9\cdot10^{-5}$MW/GeV/(MeV/m)/sec for $\tau = .35$, $\eta = 0.3$, $\nu_{rf} = 4040$ MHz and $r/Q = 9470 \, \Omega/m$).[17]

Here the factor 2 accounts for the two linacs, η is the efficiency to transform electrical into rf power, τ is the attenuation constant of the accelerating structure, and $\omega_{rf}(r/Q) \sim \omega_{rf}^2$ rf frequency-related parameters.

We will use Eqs. (VII.3) through (VII.8) to determine the performance of the linear collider in the next section.

Parameters and Performance of the Linear Collider

Eqs. (VII.3) through (VII.8) do not uniquely define all important parameters. We will have to fix some parameters. The selection of which can greatly influence the performance of the linear collider. We will make the following selection of free parameters:

$$P_{AC} \quad = \quad 100 \text{ MW}$$
$$g \quad = \quad 100 \text{ MeV/m}^7$$
$$\sigma_\ell \quad = \quad 2 \text{ mm} \qquad\qquad\qquad (VII.9)$$
$$\sigma_y \quad \geqslant \quad 0.4 \text{ }\mu m$$
$$\nu_{rf} \quad = \quad 4040 \text{ MHz}^7$$

We still have to decide on the number of particles per bunch. According to Eq. (VII.7) the value for N can be raised as the injection energy E_o into the linac is increased. This can be done by the following trick. Assume we have an accumulator storage ring of say E_o = 10 GeV. A preceeding 10-GeV linac produces pulses of lower intensity N_o (limited only by wake fields) at a rate ν_{repo} much faster than the pulse repetition rate ν_{rep} of the main linac. These are stored in the accumulator storage ring. The resulting high intensity bunches are then extracted to the linac. As long as we have the relation $\nu_{repo} N_o \geq \nu_{rep} N$ the scheme works. In Table VII.1 an example of an accumulator storage ring matched to the requirements of the linear collider is shown. The maximum intensity N_o of particles in the fast cycling linac can be determined by experiments like those being performed at SLAC in connection with the SLC program.

Table VII.1

Energy	E_o	=	10 GeV
Damping ring	τ_x	=	1.75 msec
Bending radius	ρ	=	43 m
Circumference	C	=	540 m
Total rf power	P_{rf}	=	1 MW
Beam emittance	$\epsilon\gamma$	=	3×10^{-5} m
Energy spread	σ_E/E	=	0.13%

The parameters of Table VII.1 are entirely feasible and do not pose any problem.

The last free parameter we want to choose is the energy spread $\Delta E/E$ due to beam strahlung. The allowable energy spread will be limited by the resolution required in the high-energy physics experiments. At very high energies, however, no phenomena are expected that require a very good energy resolution. Since the allowable energy spread has some influence on the achievable luminosity, it will be chosen so as to maximize the luminosity. By now all parameters in Eqs. VII.3 through VII.8 are either fixed or determined by the equations and Fig. VII.1.

In Fig. VII.2 we show the luminosity arrived at by the assumptions just made as a function of energy. For the energy spread due to beam strahlung we have assumed $\Delta E/E$ = 0.03 and 0.10. In the case of $\Delta E/E$ = 0.10 we have a luminosity of more than $10^{33} \text{cm}^{-2}\text{sec}^{-1}$ up to $E_{c.m.}$ = 1000 GeV. The luminosity now is limited purely by the electrical power and can be changed proportional to that power.

By manipulation of Eqs. VII.3 through VII.8 we can express the luminosity in terms of quantities determined by external rather than fundamental limitations and get:

$$\mathscr{L} = \left(\frac{3mc^2}{32\pi^2 r_e^3} \right)^{\frac{1}{2}} \left(\frac{A}{\sqrt{f}\ \alpha} \right) \left(\frac{\Delta E}{E}\ \sigma_\ell \right)^{\frac{1}{2}} \frac{N_b P\ K_o\ P_{AC}}{E^{3/2} \sigma_y \ln E/E} \qquad (VII.10)$$
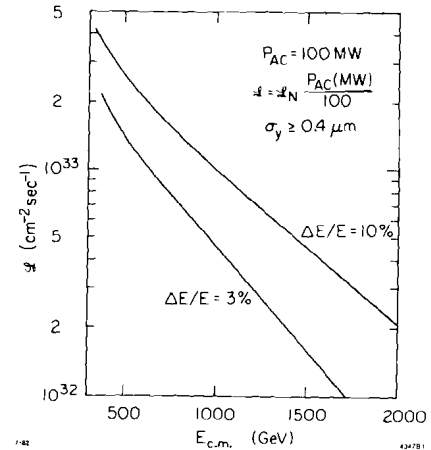

Fig. VII.2: Luminosity

Here we have used the approximation F(R) = f/R which is a good representation of Eq. VII.6 for R >> 1 and f ≈ 1.07. In the examples of this note the values for R vary between 5 and 10 for $\Delta E/E$ = 10% and between 8 and 19 for $\Delta E/E$ = 3%. This relation clearly exhibit the scaling of the luminosity with various free parameters. Specifically we note for P_{AC} = const that

$$\mathscr{L} \sim \sqrt{\Delta E/E} \qquad\qquad (VII.11)$$

$$\mathscr{L} \sim E^{-3/2} \qquad\qquad (VII.12)$$

and

$$\mathscr{L} \sim 1/\sigma_y \qquad\qquad (VII.13)$$

The last relation tell us to reduce the vertical beam size as much as possible. The lower limit of the beam height σ_y will be set at any time by the state of the art for the stability in time of most of the component of a linear collider like power supplies, ground motion etc. Fig. VII.3 does not show a pure linear dependence on σ_y since we have chosen $\sigma_y \sim E^{-\frac{1}{2}}$ reflecting the adiabatic damping.
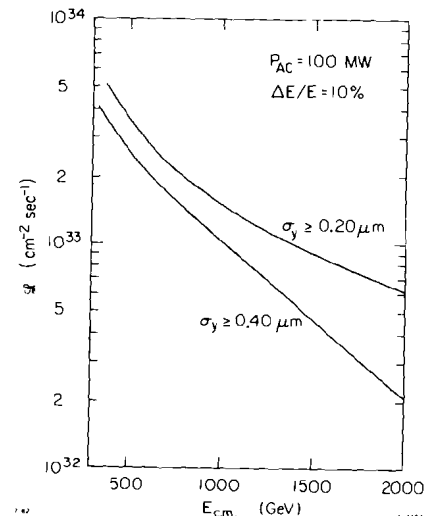

Fig. VII.3: Luminosity for Different Beam Heights

We also note from Eq. VII.10 that in order to keep the luminosity constant we have to raise the

electrical power like

$$P_{AC} \sim E^{3/2} \qquad\qquad (VII.14)$$

The simple relations VII.11 through VII.14 are not
exact since by changing any parameter we also change
the disruption parameter D and therefore change the
luminosity enhancement factor. The errors, however,
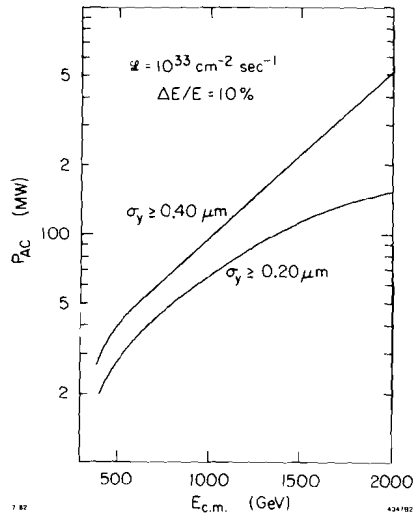are too small to change the general scaling.

Fig. VII.4: Electrical Power Versus
Energy for Constant
Luminosity.

Conclusion

From a technical point of view a linear collider
of high energy and luminosity cannot be operated
economically at the present date. A series of R&D
efforts in different areas are required to produce the
necessary technology for an economically feasible
linear collider. No fundamental limits, however, have
been found as yet that would prevent us from reaching
the goals outlined in this report. Most of the
critical component will be tested in a "real like"
situation once the SLC[18] comes into operation. Beyond
that much R&D is required in rf-power sources to re-
duce the power consumption and in high gradient accel-
erating structures to minimize the required real
estate and linear construction costs.

References

1. Proceedings, SLC Workshop (SLAC-247), March 1982; Summer Study 1979; Proceedings, Cornell Z^0 Workshop, February, 1981.

2. (a) J. Ellis, e^+e^- Physics Beyond LEP, Proceedings of the IFCA Workshop, 1980, Switzerland.

   (b) C. H. Llewellyn Smith, e^+e^- Physics Beyond PETRA Energies, LEP Summer Study 10-22, September 1978.

   (c) I. Hinchliffe, Vector Meson Backgrounds at High Energy e^+e^- Machines. To be published in these proceedings.

3. "The Scalar Sector of Electroweak Interactions", Report of the Higgs and Technicolor Subgroup of the Beyond the Standard Model Group, in these Proceedings.

4. G. R. Farrar and P. Fayet, Phys. Lett. 89D, 191 (1980).

5. I. Hinchliffe, Phonomenological consequences of Supersymmetry. To be published in these Proceedings.

6. For a review of Composite Models, see M. Peskin in the Proceedings of the 1981 International Symposium on Lepton and Photon Interactions at High Energies, W. Pfiel editor (Bonn., 1981). In many models, one expects $\Lambda \simeq$ 1-100 TeV.

7. E. Eichten, K. Lane and M. Peskin, "New Tests of Quark and Lepton Substructure", to be submitted to Physical Review Letters.

8. See also: Report of the Compositeness Subgroup of the Beyond the Standard Model Group, M. Peskin organizer (in these Proceedings); H. Kagan, New Particles Near the Z^0, in Report of the 100 GeV Facility Subgroup of the e^+e^- Collider Group (in these Proceedings). Other tests of Quark and Lepton Compositeness in e^+e^- Annihilation are discussed here and in Ref. 2.

9. I am grateful to H. Kagan for useful discussions and suggestions on this Measurement and for help in Computing Λ_{ee}.

10. J. A. Vermaseren et al., Phys. Rev. D19, 137 (1979) and references therein.

11. M. Tigner, Nuovo Cimento 37, 1228 (1965).

12. Proc. of the Workshop on Possibilities and Limitations of Accelerators and Detectors, Fermilab, Batavia, (1979).

13. Proc. of the 2nd ICFA Workshop on Possibilities and Limitations of Accelerators and Detectors, Les Diabletets, (1979).

14. U. Amaldi, International Symposium on Lepton and Photon Interactions at High Energies, Fermilab, Batavia, (1979).

15. H. Wiedemann, Proc. of the Summer School on Particle Physics, Stanford (1981).

16. B. Richter, Proc. of the 1981 Summer School on High Energy Particle Accelerators, Femilab, Batavia, (1981) (to be published).

17. P. Wilson, Proc. of the 1981 Summer School on High Energy Particle Accelerators, Fermilab, Batavia, (1981)(to be published).

18. SLAC Linear Collider Conceptual Design Report, SLAC-229, (1980).

19. I. F. Ginzburg et al., Novosibirsk (1981), Preprint 81-102.

20. R. Hollebeek, Nucl. Instrum. Methods 184, 333 (1981).

21. H. Bassetti and M. Gygi-Hanney, LEP-NOTE-221, (1980).

22. A. Chao, C. Y. Yao, B. Richter NIM 178, 1 (1980).

23. A. Chao pointed out that Eq. (3.5) also involves the focusing along the linac with $N \sim 1/L_Q$, where L_Q is the distance between quaduroles. Eq. (3.5) assumes $L_Q = 12.5$ m (SLC). This distance certainly can be reduced and the luminosity $\sim 1/L_Q$ increased or other critical parameters relieved.

24. M. Davier, LEP Summer Study/I-3 Fig. 6, Sept. 1978.

Di-jet Mass

As a model consider the production of $W^{\pm}$ pairs at 700 GeV CM energy, with each W decaying into two jets. Ignore particle masses in the jet (mostly π's). The W will look like a $\pi^o \to 2\gamma$'s. Then at the min. opening angle

$$M^2(\text{di-jet}) = 2 \, E^2 (1 - \cos \theta).$$

Min. opening angle $\theta \simeq \dfrac{2 \, M_W}{E_W} = 25.5^o$

$$\frac{\Delta M}{M} = \sqrt{\left(\frac{\Delta E}{E}\right)^2 + \left(\frac{\Delta \theta}{\theta}\right)^2}$$

where : E = single jet energy, ΔE the energy measurement error, $\Delta \theta$ the single jet angular error (1/2 angle of error-cone).

The SLC workshop results have shown that the direction of a jet can be measured with an error of $\sim \pm$ 25 m.r., using electromagnetic and hadronic calorimetry. They also showed that $\sim$ 30% of jet energy is electromagnetic and the rest is hadronic.

Using calorimetry similar to the SLC i.e. with

$$\left(\frac{\Delta E}{E}\right)_{e.m.} = \frac{15\%}{\sqrt{E}} \quad , \quad \left(\frac{\Delta E}{E}\right)_{had} = \frac{50\%}{\sqrt{E}} \quad , \text{ and using}$$

the energy division above, then in our case:

$$\left(\frac{\Delta E}{E}\right)^2_{jet} \approx 1 \times 10^{-3}$$

$$\left(\frac{\Delta \theta}{\theta}\right)^2 \approx 3.5 \times 10^{-3}$$

This gives $\dfrac{\Delta M}{M} \approx 7\%$. (See Fig. A.1)

This estimate is optimistic because of a small loss of energy in undetected particles, and pessimistic because the angular error dominates and we calculated it at min. opening angle.

It is interesting to compare this with $\dfrac{\Delta M}{M}$ for a .5 GeV π^o in the crystal ball at SPEAR $\dfrac{\Delta E}{E} \approx 2.8\%$,

$\dfrac{\Delta \theta}{\theta} \approx 5\% \to \dfrac{\Delta M}{M} \approx 6\%$.

The situation is better for the case of $\geq$ 4W's sharing 700 GeV equally because the min. opening angle is larger and hence the dominating angular error is smaller.
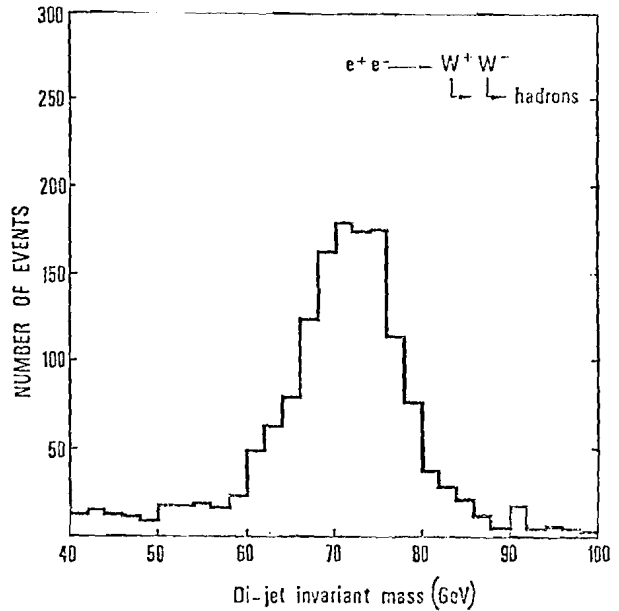

Fig. A.1: Di-jet invariant mass distribution in $e^+e^- \to W^+W^-$ each decaying into 2 jets. Jet energy and angle are measured in a fine-grain calorimeter. Only the combinations with E(Tot) equal to beam energy are plotted. From Ref. 24.

$e^+e^- \to$	R σ/σ_{pnt}	Particle Decay	Jet (Max) Content	REMARKS
W^+W^- Z^oZ^o $Z^o\gamma$	~ 25 ~ 5 ~ 30	Jet & Leptons	4 4 2 + SHWR	With known W's and Z^o, this constitutes a serious background. However ang. dist. is strongly peaked forward - backward, also Z's, W's can be used as a tag. $Z^o\gamma$ can be easily recognized and eliminated.
Known Quarks $Q(2/3)\bar{Q}$ $Q(-1/3)\bar{Q}$ Total	 ~ 2 ~ 1 ~ 9.0	Jets "	 2 2	Includes Z^o contribution as well as γ. They also complicate analysis due to gluons, hence are also a background. However the two jets are back to back.
New Res. $Z^{o'}(M \geq$ 200 GeV)	5000	Like Z^o		Assume coupling similar to Z^o. $\Gamma'/M' = \Gamma/M(Z^o)$ $\sim 3\%$. To study very well E-beam resol. should be better than 3%.
New Onia $n\ ^3S_1$	$1 \to 2$	ψ, ψ'Like	2 almost b-to-b	Will have substantial weak decay $q' \to W + q$, $H + q$. $\Gamma(q' \to W + q) \approx 6 \times 10^{-3} M_q'$. Separation of two oniums $\approx 5 \times 10^{-3} M_q'$. Hence resonance is broadened. Most promising detection is by R steps at threshold and sphericity above threshold, and by jump in W^+W^- from weak decay.
Techni-colour $\rho_T(M \geq$ 700 GeV)	~ 10	$\rho_T \to \pi_T\pi_T$ $\rho_T \to$ Long. Pol. Z, W	4	ρ_T is supposed to be very wide. Its tail might be seen at E_{cm} 700 GeV or less. π_T also looks like a Higgs. $M(\pi_T)(10 \to 100)$. See Fig. 1 for estimates in two models, and Ref. 3 for more details.
New Higgs $Z^o + H^{o'}$ $M(H^{o'}) \approx$ 200 GeV	.16 @ M = 200	$H^{o'} \to Z^oZ^o$ W^+W^-	6	Can be produced up to kin. lim. $M_{H^{o'}} = E_{CM} - M_{Z^o}$. The Z^o or $W^\pm$ can be used as a tag. Inv. mass of di-jet is needed. New Higgses can be accommodated in the standard model. Study of Higgs is best at high energies.
$H^{'+} H^{'-}$	$.3\ \beta^3$	$H' \to$ heavy q - pairs	4 to 6	β^3 factor requires energies above H' mass. Di-jet mass is needed. H^+H^- has $\sin^2\theta$ distribution. The No. of jets depends on quark masses.
Sup. Symm $\tilde{q}\ \tilde{\bar{q}}$	$u\ \tilde{u}$ } ~ 1 } $d\ \tilde{d}$ } $\sim .5$ }	$\tilde{q} \to q + \tilde{\gamma}$ $\tilde{q} \to q + \tilde{g}$ $\tilde{g} \to q\ \bar{q}\ \tilde{\gamma}$	6	In that case we get two jets back to back almost with some missing energy. β^3 factor and $\sin^2\theta$ for $\tilde{q}\ \tilde{\bar{q}}$.
$\tilde{\ell}^+ \tilde{\ell}^-$ $W^\pm \tilde{\ell}^\pm$ $\ell_o + \tilde{\ell}_o$	.52 .14	$\tilde{\ell} \to \tilde{\gamma}\ \ell^\pm$ $\tilde{\gamma}$ is un-seen	2	These are scalar leptons. They behave like scalar quarks with q replaced by ℓ. The energy scale for super symm. might be like weak interactions ~ 100 GeV. Note β^3 fact-and $\sin^2\theta$ distribution.
$\tilde{W}^+ \tilde{W}^-$ } ($q\ \bar{q}\ \tilde{g}$ + $\bar{q}\ \bar{q}\ \tilde{g}$)	~ 2			These are supposed to be leptons with spin 1/2. See Reference 5.
$e^+ e^- \to$ $e_c^+ e_c^-$	Depends on scale Λ			Can place limits on electron's inverse size $\Lambda > 16$–30 TeV. At $\sqrt{s} \sim \Lambda$, $\sigma(e^+e^- \to e^+e^-) \sim 1/\Lambda^2$, a "strong" interaction cross-section.

TABLE II.

State	Z^0	ρ_T	H'	H.Q	Rest[*]	Rest(cos $\theta \leq$ .8)[**]
R	$\sim$ 5000	$\sim$ 10-20	$\sim$ .5	$\sim$ 2	$\sim$ 35	$\sim$ 20
N/Day @ $\mathscr{L} = 10^{33}$	75000	150-300	8	30	525	300

[*] 25 units of R for uncut $W^+ W^-$, $Z^0 Z^0$ (see Ref. 2 (c)), 10 units of known quarks, 4 units for supersymmetric particles.

[**] $W^+ W^-$, $Z^0 Z^0$ after cuts for solid angle (Ref. 2 (c)) give 5 units. Remainder (14 units) left uncut.